THE JOURNAL OF BIOLOGICAL CHEMISTRY VOL. 288, NO. 30, pp. 21742–21754, July 26, 2013

α-Synuclein Oligomers Impair Neuronal Microtubule-Kinesin Interplay*[S]

Received for publication, January 9, 2013, and in revised form, May 16, 2013 Published, JBC Papers in Press, June 6, 2013, DOI 10.1074/jbc.M113.451815

Iryna Prots[‡], Vanesa Veber[‡1], Stefanie Brey[‡1], Silvia Campioni[§], Katrin Buder[¶], Roland Riek[§], Konrad J. Böhm[¶], and Beate Winner[‡2]

From the [‡]Junior Research Group III, Interdisciplinary Centre of Clinical Research, Nikolaus Fiebiger Centre for Molecular Medicine, Universitaetsklinikum Erlangen, Glueckstrasse 6, 91054 Erlangen, Germany, the [§]Laboratory of Physical Chemistry, HCI F 225, Swiss Federal Institute of Technology Zurich, Wolfgang-Pauli-Strasse 10, 8093 Zurich, Switzerland, and the [¶]Leibniz Institute for Age Research-Fritz Lipmann Institute e.V., Beutenbergstrasse 11, 07745 Jena, Germany

Background: α-Synuclein aggregates cause early neurite pathology by as yet unknown mechanisms.
Results: α-Synuclein oligomers and seeds decrease microtubule stability, kinesin-microtubule interaction, cellular cargo distribution, and neurite network morphology.
Conclusion: Various α-synuclein species interact differently with proteins of axonal transport.
Significance: The impairment of the microtubule-kinesin function by α-synuclein oligomers drives early neurite pathology.

Early α-synuclein (α-Syn)-induced alterations are neurite pathologies resulting in Lewy neurites. α-Syn oligomers are a toxic species in synucleinopathies and are suspected to cause neuritic pathology. To investigate how α-Syn oligomers may be linked to aberrant neurite pathology, we modeled different stages of α-Syn aggregation *in vitro* and investigated the interplay of α-Syn aggregates with proteins involved in axonal transport. The interaction of wild type α-Syn (WTS) and α-Syn variants (E57K, A30P, and aSyn(30–110)) with kinesin, tubulin, and the microtubule (MT)-associated proteins, MAP2 and Tau, is stronger for multimers than for monomers. WTS seeds but not α-Syn oligomers significantly and dose-dependently reduced Tau-promoted MT assembly *in vitro*. In contrast, MT gliding velocity across kinesin-coated surfaces was significantly decreased in the presence of α-Syn oligomers but not WTS seeds or fibrils (aSyn(30–110) multimers). In a human dopaminergic neuronal cell line, mild overexpression of the oligomerizing E57K α-Syn variant significantly impaired neurite network morphology without causing profound cell death. In accordance with these findings, MT stability, neuritic kinesin, and neuritic kinesin-dependent cargoes were significantly reduced by the presence of α-Syn oligomers. In summary, different α-Syn species act divergently on the axonal transport machinery. These findings provide new insights into α-Syn oligomer-driven neuritic pathology as one of the earliest events in synucleinopathies.

α-Synuclein (α-Syn)[3] is a 140-amino acid membrane-binding protein widely distributed in brain tissue (1). Its exact physiological role remains unclear, but due to its presynaptic localization, a role in the regulation of neurotransmitter release was shown (2). Multiplications and missense point mutations (A30P, E46K, and A53T) in the α-Syn gene cause an early onset of familial forms of Parkinson disease (PD) and strongly link α-Syn with the pathogenesis of PD (3–6). Moreover, deposits mainly composed of α-Syn fibrils either in the cytoplasm (Lewy body) or in neurites (Lewy neurite) are the pathologic hallmarks of synucleinopathies, including sporadic PD and dementia with Lewy bodies (7, 8). In the process of aggregation of α-Syn, soluble oligomers, protofibrils, and insoluble amyloid fibrils are formed (9). Although cytotoxicity *in vitro* and *in vivo* is currently attributed to oligomers of α-Syn rather than to fibrils (10–13), the temporal and molecular mechanisms underlying α-Syn aggregation-driven neurodegeneration are far from understood.

There is increasing evidence for a direct interplay between α-Syn aggregation and axonal transport. Axonal transport relies on the microtubule (MT) network and on the MT-based motor proteins, kinesin and dynein, and is fundamental for the maintenance of neuronal homeostasis (14). A decline in axonal transport motor proteins was reported in sporadic PD brains, and this decline correlated with the presence of α-Syn aggregates (15). Furthermore, overexpression of α-Syn oligomeric mutants resulted in neurite swellings in rat substantia nigra neurons (13). The interaction of α-Syn with tubulin and MTs was shown *in vitro* and *in vivo*, and α-Syn overexpression and aggregation was associated with disrupted MT networks (16–22). Together, these data strongly suggest alterations in the intracellular transport machinery in synucleinopathies. Although α-Syn oligomers were implicated in decreased tubulin polymerization in a cellular model (23), the specific relation of oligomers/fibrils and

* This work was supported by ELAN (Erlanger Leistungsbezogene Anschubfinanzierung und Nachwuchsföderung) Fonds Grant 11.08.19.1 (to I. P.); the Interdisciplinary Center for Clinical Research (IZKF N3, Universitaetsklinikum Erlangen); the Bavarian Ministry of Sciences, Research, and the Arts in the framework of the Bavarian Molecular Biosystems Research Network (BioSysNet); and German Federal Ministry of Education and Research (BMBF) Grant 01GQ113.
[S] This article contains supplemental Movies 1 and 2.
[1] Both authors contributed equally to this work.
[2] To whom correspondence should be addressed. Tel.: 49-9131-85-39301; Fax: 49-9131-85-39311; E-mail: beate.winner@med.uni-erlangen.de.

[3] The abbreviations used are: α-Syn, α-synuclein; PD, Parkinson disease; MT, microtubule; WTS, wild type α-Syn; MTP, microtubule protein; MAP, microtubule-associated protein; LUHMES, Lund human mesencephalic; LV, lentiviral; MOI, multiplicity of infection.

different compartments of the neuronal cytoskeletal machinery has not yet been elucidated.

In the present study, we used recombinant α-Syn protein (wild type, single point mutants, and the fragment 30–110) to obtain different aggregate species *in vitro* and evaluated the direct effect of these species on MT polymerization and kinesin-dependent MT gliding in a cell-free system. Our data showed that α-Syn oligomers have a strong influence on kinesin-driven MT motility, whereas seeds of α-Syn significantly inhibited MT assembly, promoted by the axon-specific MAP, Tau. In a cellular system, mild overexpression of an oligomerizing α-Syn variant and, less potently, α-Syn seeds impaired neurite network morphology. This was accompanied by impaired MT stability and reduced presence of kinesin and kinesin-dependent cargoes within neurites. Our results suggest that the MT-kinesin network is the first target of soluble α-Syn aggregates.

EXPERIMENTAL PROCEDURES

α-Syn Preparation—α-Syn wild type (WTS) and the α-Syn variants E57K (glutamic acid to lysine substitution at amino acid 57 of the α-Syn protein), A30P (alanine to proline substitution at amino acid 30 of the α-Syn protein), and aSyn(30–110) (core part of the α-Syn protein consisting of amino acids 30–110) were used. WTS and all α-Syn variants were expressed in *Escherichia coli*. α-Syn protein purification was performed with a modified version of previously published protocols taking advantage of several protein precipitation steps (13, 24). Briefly, the pellet obtained in the 50% (v/v) ethanol precipitation step was resuspended in 9 ml/liter of culture of 20 mM Tris, pH 8, and dialyzed overnight at 4 °C against the same buffer with a 3.5-kDa cut-off membrane (Spectrum Laboratories Inc., Rancho Dominguez, CA). The sample was applied onto a HiTrap Q HP column (GE Healthcare), equilibrated with 20 mM Tris, pH 8, and eluted with a linear gradient from 0 to 500 mM NaCl over 10 column volumes. The collected fractions were analyzed by SDS-PAGE and Coomassie Brilliant Blue staining, and α-Syn-containing fractions were merged. For aSyn(30–110), the flow-through was collected, analyzed by SDS-PAGE, and concentrated with 3-kDa cut-off Amicon concentrators (Merck Millipore, Darmstadt, Germany). All preparations were finally dialyzed against 20 mM ammonium acetate, lyophilized, and stored at −20 °C. The lyophilized samples were resuspended in MT assembly buffer (20 mM PIPES, 80 mM NaCl, 1 mM EGTA, 0.5 mM $MgCl_2$, pH 6.8) at a concentration of 400 μM and stored at −20 °C until usage. The purity of α-Syn proteins was 98–100%, as determined by SDS-PAGE followed by Coomassie Brilliant Blue staining (data not shown).

α-Syn Aggregation—400 μM α-Syn solutions were diluted to 100 μM solutions with MT assembly buffer before aggregation. One part of each 100 μM α-Syn protein solution was left untouched and was considered as a monomer fraction. The rest was transferred to a multimer fraction, applying a previously published protocol (13) with some modifications: incubation at 37 °C for 12 h followed by 56 °C for 16 h with slight agitation.

Electron Microscopy (EM) of α-Syn Multimers—The samples for negative stain transmission EM were prepared at the completion of the aggregation protocol. 3 μl of the 100 μM α-Syn multimer solutions were adsorbed onto 100-mesh Formvar/carbon-coated copper grids (Plano GmbH, Wetzlar, Germany), briefly washed with distilled water, and negatively stained with 1 g/100 ml of aqueous uranyl acetate for 1 min. Grids were analyzed on a transmission electron microscope (JEM 1400, Jeol, Tokyo, Japan). Digital images were taken using a CCD-Camera Orius SC1000 (Gatan Inc., Pleasanton, CA).

Preparation of Microtubule Proteins and Kinesin—In the present study, full-length human neuron-specific kinesin-1 ($KIF5A_{full}$) and its truncated form comprising 560 amino acids from the N terminus and containing the motor domain, neck, and part of the stalk ($KIF5A_{560}$) were used. Kinesins were expressed in *E. coli* as fusion proteins with a C-terminal chitin-binding intein tag and purified by binding to chitin beads followed by removal of the intein tag by 50 mM DTT-induced specific self-cleavage (25). The kinesins were stored in motility buffer (50 mM imidazole, 0.5 mM $MgCl_2$, 0.5 mM EGTA, 0.5 mM DTT, pH 6.8) supplemented with 150 mM NaCl and 1 M glycerol at −80 °C.

Microtubule protein (MTP) consisting of 80% tubulin and 20% complete MAP set (MAP1, MAP2, and Tau) was purified from porcine brain homogenates by two cycles of temperature-dependent disassembly (0 °C)/reassembly (37 °C) (26). To obtain pure tubulin, co-purified MAPs were removed by phosphocellulose ion exchange chromatography, according to a previously published protocol (27). MAP2 and Tau were eluted from the phosphocellulose, treated for 5 min at 95 °C (28), and separated from denatured material (MAP1 and residual tubulin) by ultracentrifugation (45 min, 40,000 rpm, Beckman Coulter Ti50.2 rotor, Beckman Coulter, Krefeld, Germany). Tau and the high molecular weight MAP2 were separated by passing the clear supernatant through a 100-kDa ultrafilter. All proteins (*i.e.* MTP, tubulin, MAP2, and Tau) were frozen in liquid nitrogen and stored at −80 °C until usage.

Stabilized MTs were formed by taxol-promoted self-assembly at 37 °C from 2 mg/ml pure tubulin in the MT assembly buffer supplemented with 0.2 mM GTP and 20 μM taxol. MTs were usually prepared at the day of usage at least 30 min prior to an experiment. The purity of kinesins was 75–80%, and the purities of MTP, tubulin, MAP2, and Tau were all 95–98%, as determined by SDS-PAGE followed by Coomassie Brilliant Blue staining.

Ligand Blot—Cytoskeleton proteins (total amount of 1 μg/spot) were dotted onto nitrocellulose membrane stripes in the order shown in Fig. 1. BSA was used to control for a non-specific binding of α-Syn. As positive control, 3 μl of 100 μM α-Syn solution were applied. Proteins were allowed to bind to the nitrocellulose for 5 min at room temperature. Unbound proteins were removed by washing three times with a blocking buffer (0.5 g/100 ml BSA, 0.5% Tween 20 in PBS). All further washing steps and antibody dilutions for ligand blot experiments were performed in the blocking buffer. The stripes were incubated in 10 μM solutions of monomeric or multimeric WTS or α-Syn variants overnight at 4 °C. To control for non-specific binding, one stripe was incubated in the blocking buffer in the absence of α-Syn. Unbound α-Syn was washed out three times. α-Syn binding was detected after incubation with monoclonal mouse anti-α-Syn antibody (1:1000; clone 42, BD Biosci-

ences) for 1 h at room temperature followed by three times washing and incubation with goat anti-mouse antibody labeled with an infrared dye, IRDye 800CW (1:2000; LI-COR Biosciences, Lincoln, NE) for 1 h at room temperature. After extensive washing, the stripes were developed on the Odyssey infrared imager using the Odyssey application software version 3.0 (both from LI-COR Biosciences). Densitometry analysis was performed by estimating an integrated intensity value of each spot that is proportional to the amount of dye-labeled antibodies on the membrane using the Odyssey application software. Three independent ligand blots were performed, and mean values of the intensities ± S.D. were calculated.

Microtubule Assembly Assay—MT assembly was recorded at 37 °C by a Cary 100 spectrophotometer equipped with a temperature-controlled multicell holder (Agilent Technologies, Böblingen, Germany) using 2-mm OS glass cuvettes (Hellma GmbH & Co. KG, Müllheim, Germany). For this, the proteins were adjusted to a total volume of 275 μl in the MT assembly buffer containing 0.5 mM GTP.

To analyze the influence of α-Syn on MT polymerization in the presence of MAPs, assembly was performed 1) from MTP (final concentration 1.3 mg/ml) in the presence of 4 μM WTS or α-Syn variants; 2) from pure tubulin (16 μM) with MAP2 (1.6 μM) in the presence of 6.3 μM WTS or α-Syn variants; or 3) from pure tubulin (16 μM) with Tau (2.1 or 2.7 μM) in the presence of 8.7 μM WTS or α-Syn variants. To investigate if there is a dose-dependent effect of WTS on Tau-promoted MT assembly, WTS was added to the assembly reaction (16 μM tubulin and 2.1 μM Tau) at concentrations of 2.18, 4.36, 8.73, and 17.45 μM. As a control, MTs were assembled at the respective conditions in the absence of α-Syn. As a negative control for MT polymerization, MT assembly was performed from purified tubulin (16 μM) with or without α-Syns (6.3 μM) and in the absence of any MAPs. The MT assembly measurements with MAP2 and MTP were performed with an additional cooling step to 10 °C. The rationale for the cooling step was to test for a possible stabilizing effect of α-Syn on established MT in the absence of the α-Syn inhibitory effect on MT polymerization. Measurements of Tau-promoted MT assemblies were performed with an addition of the MT assembly-promoting drug taxol to a final concentration of 10 μM. The rationale for the taxol step in Tau assemblies was to prove that tubulin had not lost its assembling capacity under α-Syn-inhibitory conditions. MT polymerization was measured as the turbidity ($A_{360\ nm}$) of the solution recorded every 4 s at 360 nm over 30–60 min. Data are shown as representative assembly curves and mean assembly levels at 30 min (plateau level, representing the assembly/disassembly steady state) of three independent experiments for each condition. To quantitatively analyze the effect of α-Syns on MT assembly, the turbidity signals after 30 min in each assay were compared with that of the control condition.

In Vitro Gliding Assay—Gliding assays were performed on glass slides (for principles, see Ref. 29) covered by casein (5 mg/ml). MT were assembled and stabilized as described above. All gliding assays were performed with the $KIF5A_{560}$ in the motility buffer supplemented with 20 μM taxol. The gliding assay mixture containing $KIF5A_{560}$ (0.4 mg/ml), stabilized MTs (40 μg/ml), 100 mM NaCl, 0.5 mM ATP, and 10 μM α-Syn was incubated for 5 min at room temperature prior to transfer onto the casein-coated glass slide. The sample was covered by a coverslip, and MT gliding was observed as described below. The control gliding assay was performed in the absence of α-Syn. MT gliding velocities were measured during observation by following the tracks of individual MTs using the Argus-20 software (Hamamatsu Photonics, Herrsching am Ammersee, Germany). All gliding assays were carried out at 36 °C. The mean gliding velocities were calculated from the gliding velocities of at least 10 MTs in each sample.

Gliding Assay Microscopy and Data Analysis—MT gliding was visualized by video-enhanced differential interference contrast microscopy. All analyses were performed using an Zeiss Axiophot microscope (Carl Zeiss, Munich, Germany) equipped with a Plan-Neofluar ×63/1.25 oil immersion objective (Carl Zeiss), a Chalnicon video camera type C2400-0.1 (Hamamatsu Photonics), and the image processing system Argus-20 (Hamamatsu Photonics), which enables background subtraction and electronic contrast enhancement. MT movement was documented on a digital hard disk recorder (JVC SR-DVM70EU, JVC, Wayne, NJ). Video sequences were digitized using Adobe Photoshop, resulting in image sequences of 30 frames/s.

Lund Human Mesencephalic (LUHMES) Cell Culture—LUHMES cells (gift of Dr. M. Leist, Konstanz, Germany; described in Ref. 30) were cultured at 37 °C in a humidified 95% air, 5% CO_2 atmosphere. Cells were cultured in plastic flasks or in plastic plates coated with poly-L-ornithine (50 μg/ml) and fibronectin (1 μg/ml) (both from Sigma-Aldrich) overnight at 37 °C and washed once with PBS prior to seeding the cells. LUHMES cells were maintained and expanded in advanced DMEM/F-12/Glutamax medium supplemented with N2 supplement (both from Invitrogen) and 40 ng/ml FGF2 (R&D Systems, Wiesbaden-Nordenstadt, Germany) in flasks. Cells were split using TrypLE Express (Invitrogen) at 80% confluence. Neuronal differentiation of LUHMES cells was performed for 6 days in 24-well plates (150,000 cells in 500 μl/well) in advanced DMEM/F-12/Glutamax/N2 medium supplemented with 1 μg/ml tetracycline, 1 mM cAMP (both from Sigma-Aldrich), and 2 ng/ml glial cell-derived neurotrophic factor (R&D Systems). Lentiviral (LV) constructs encoding for either WTS or the E57K α-Syn variant containing an internal ribosome entry site GFP sequence or LV encoding only an internal ribosome entry site GFP (referred to hereafter as WTS, E57K, and GFP, respectively) were used to infect LUHMES cells. LUHMES cells were predifferentiated for 2 days before infection at a multiplicity of infection (MOI) of 2 (mild) or 4 (high overexpression). LV infection was performed for 48 h.

Analysis of LUHMES Cells—At day 4 of differentiation, infected cells were either incubated with 250 nM MitoTracker_RedCMXRos (Invitrogen) for mitochondria visualization for 45 min at 37 °C before fixation or directly fixed. Cells were fixed with either 4% paraformaldehyde for 20 min at 37 °C (for β3-tubulin, α-Syn, Tau, and mitochondria detection) or 100% methanol for 10 min at −20 °C followed by 4% paraformaldehyde for 15 min at 37 °C (for acetylated tubulin and KIF5 stainings). Cells were stained with rabbit monoclonal anti-β3-tubulin antibody (1:500; clone TUJ1 1-15-79, Covance, Munich,

Germany), mouse monoclonal anti-α-Syn antibody (1:250; LB509) or rabbit polyclonal anti-Tau antibody (1:50) (both from Abcam, Cambridge, MA), or mouse monoclonal anti-acetylated tubulin antibody (1:10,000; clone 6-11B-1) or rabbit anti-KIF5 (1:100) (both from Sigma-Aldrich) and were counterstained with DAPI (1 μg/ml). The following secondary antibodies were used: donkey anti-rabbit AlexaFluor546 and donkey anti-mouse AlexaFluor649 (both from Invitrogen). Cells were visualized on a Zeiss AxioVert 200 inverted microscope with the Axiovision Software (Carl Zeiss). Cell death was visualized by the addition of 0.4 g/100 ml trypan blue and was determined as a percentage of trypan blue-positive cells within a total number of cells on a particular image. Network morphology was characterized by the number of neurites crossing three unified random horizontal parallel lines over the image. Acetylated tubulin was quantified by the fluorescence intensities over the picture and normalized to the number of DAPI-positive nuclei in this picture. KIF5 signals within neurites were determined by the mean intensity along the tracing of a single neurite. At least 100 neurites were analyzed for each condition. Distribution of mitochondria in neurites was defined as the number of mitochondria/μm of a neurite length. Colocalization of α-Syn with β3-tubulin and Tau was quantified by the determination of Pearson's overlap coefficient. Each condition was performed in duplicates. Image analyses were performed using ImageJ software version 1.47f (National Institutes of Health, Bethesda, MD).

Statistical Analysis—Ligand blot densitometry data were analyzed by repeated measures analysis of variance with a Dunnett post hoc test separately for α-Syn monomers and multimers. MT assembly levels and MT gliding velocities were analyzed by one-way analysis of variance using the Dunnett post hoc test for monomers and multimers separately *versus* control condition. Neuronal network morphology, cell viability, imunohistochemical results, and mitochondria distribution were analyzed by one-way analysis of variance with Tukey's multiple comparison post hoc test. Dose dependence of the WTS effect on MT assembly was analyzed by estimating a linear regression coefficient (R^2) between assembly levels at 30 min and WTS concentrations. Differences were considered statistically significant at $p < 0.05$. Statistical tests were performed using the GraphPad Prism 5 software (GraphPad Software, San Diego, CA).

RESULTS

WTS Directly Interacts with KIF5A, Tubulin, and MAPs—Previously, α-Syn oligomers were shown to be more toxic than α-Syn fibrils and were observed to cause prominent axonal swellings in dopaminergic neurons in the rat substantia nigra *in vivo* (13, 31). We therefore aimed to investigate the interaction of different aggregated states of α-Syn with proteins involved in axonal anterograde transport.

Using a ligand blot technique, WTS, E57K, A30P, and aSyn(30–110) were tested for their interaction capacity with the following: the full-length neuron-specific motor protein kinesin KIF5A ($KIF5A_{full}$), a truncated form of a KIF5A molecule (containing the first 560 amino acids ($KIF5A_{560}$)), tubulin, assembled MTs, MAP2, and Tau (Fig. 1, *B–D*). The rational for using WTS was to mimic sporadic PD. E57K is an artificial mutant known to form oligomers but rare fibrils (13). A30P is a familial mutant, also known to form oligomers, but to a lesser extent than E57K. aSyn(30–110) represents a fibril-forming artificial mutant (32). For each α-Syn protein, monomeric and multimeric forms were analyzed separately. Multimers of the α-Syn proteins formed *in vitro* were represented either by oligomers (multimers of E57K and A30P variants) or fibrils (multimers of aSyn(30–110) variant) or a mixture of oligomers and protofibrils of WTS multimers referred to hereafter as WTS seeds (Fig. 1*A*).

WTS monomers revealed binding to KIF5A (both full-length and truncated), tubulin, MTs, MAP2, and Tau. Compared with WTS, aSyn(30–110) and two oligomerizing α-Syn variants showed weaker binding to these cytoskeleton proteins (Fig. 1*C*). Notably, WTS seeds demonstrated a prominent interaction with all tested cytoskeleton proteins compared with weaker binding of oligomers and fibrils to these proteins (Fig. 1, *B* and *D*). In summary, direct binding of oligomer and fibril-forming α-Syn variants to the proteins of MT-based cytoskeleton is significantly lower compared with WTS and WTS seeds.

α-Syn Seeds Reduce Tau-promoted MT Formation—We first tested the possibility that WTS and α-Syn variants might promote MT assembly from tubulin dimers (Fig. 2*A*). Purified tubulin was not able to assemble into MTs either in the absence of MAPs (*Control* in Fig. 2*B*) or with the addition of any of the α-Syn species (Fig. 2*B*). This indicates that α-Syn does not have an intrinsic MAP-like activity. Because WTS and, less potently, α-Syn variants were found to bind MAP2, Tau, and tubulin, we checked whether α-Syn proteins and its different multimeric forms are able to affect MT assembly in the presence of MAPs. None of the α-Syn variants (either as monomers or as multimers) had an impact on MT assembly promoted by the complete MAP set or MAP2 alone; nor did they exert an MT-stabilizing activity (Fig. 2, *C* and *D*).

This led us to investigate the influence of WTS, α-Syn variants, and their multimers on MT formation in the presence of the axon-specific MAP, Tau (Fig. 3*A*). Monomeric forms of WTS and of α-Syn variants did not influence Tau-promoted MT assembly (Fig. 3, *B* and *E*; $p > 0.05$ for the assembly levels at 30 min). α-Syn seeds significantly reduced Tau-promoted MT assembly (Fig. 3, *C* and *F*, $p < 0.05$ for the assembly levels at 30 min in the presence of WTS seeds *versus* control). Interestingly, neither oligomers alone nor α-Syn fibrils were able to influence Tau-promoted MT assembly significantly (Fig. 3, *C* and *F*). To test whether the inhibitory effect of WTS seeds on Tau-promoted MT polymerization is accompanied by irreversible changes of tubulin, we used the MT assembly-promoting drug, taxol, to trigger the formation of MTs. The addition of taxol enabled MT formation in the presence of α-Syn monomers and multimers (40 min time point; Fig. 3*B* and data not shown), suggesting that the inhibition of MT assembly by WTS seeds was not due to irreversible changes of tubulin. Thus, the inhibitory effect of WTS seeds on Tau-promoted MT formation might result from the binding of Tau by WTS seeds. To prove this possibility, MT formation was performed using higher amounts of Tau (2.7 μM instead of 2.1 μM). Indeed, at a higher Tau/WTS ratio (1:3), MTs were efficiently assembled despite

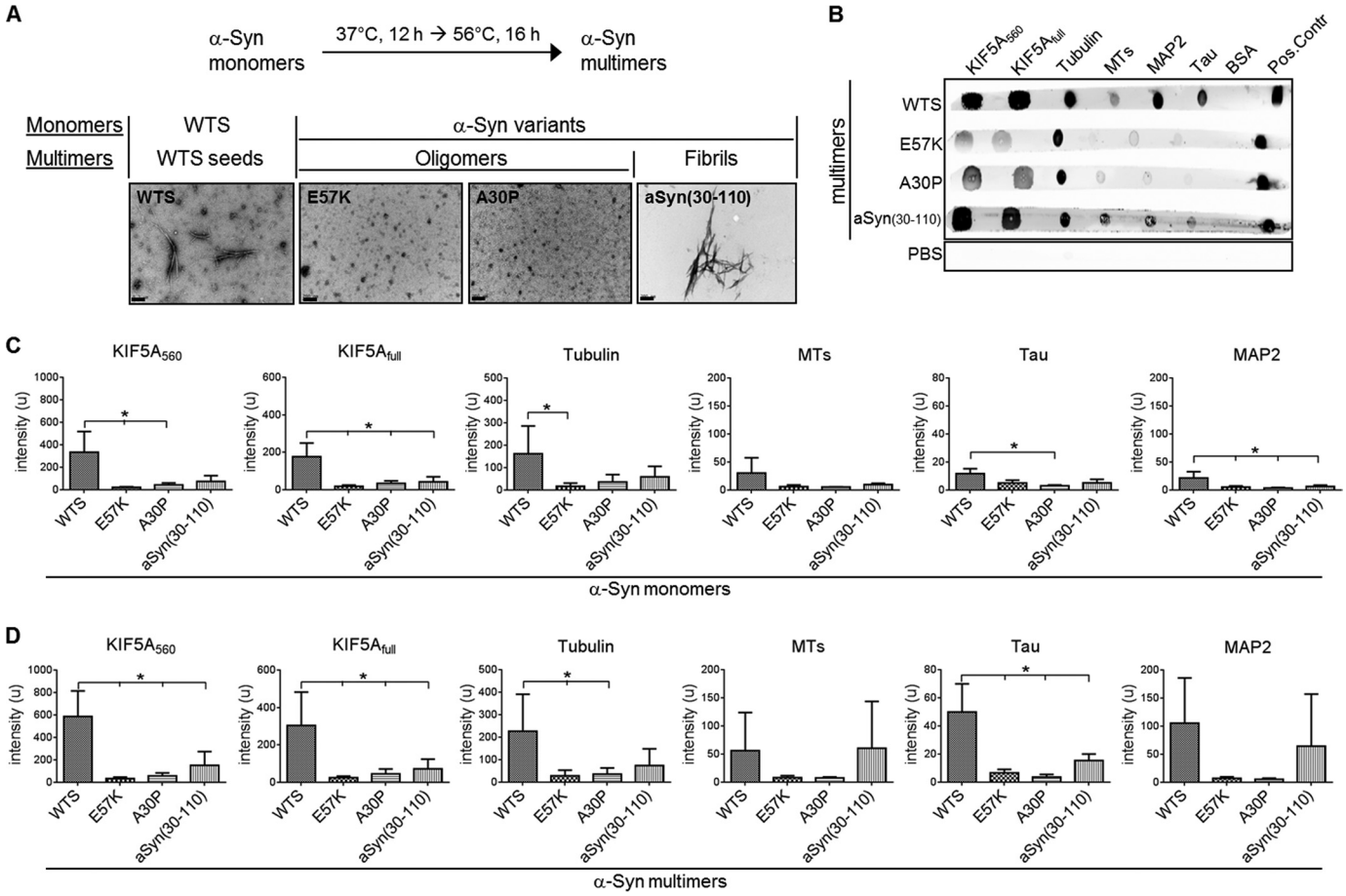

FIGURE 1. **WTS binds directly to cytoskeleton proteins.** *A*, scheme of the α-Syn *in vitro* aggregation protocol to generate α-Syn multimers (*top*). Multimers of WTS and different α-Syn variants were analyzed by electron microscopy (*bottom*). *Scale bar*, 200 nm. Nomenclature of different monomeric and multimeric α-Syn forms is shown (*bottom*). *B*, representative ligand blot performed by spotting 1 μg of the respective cytoskeleton proteins onto the nitrocellulose membrane strip. BSA was used as a negative control. 3 μl of 100 μM α-Syn solution served as a positive control (*Pos. Control*). Each strip was incubated in 100 μM α-Syn multimer solution and developed with anti-α-Syn antibody and fluorescently labeled secondary antibody. α-Syn proteins are shown on the *left*. *PBS*, the stripe that was incubated in PBS instead of α-Syn solution. *C* and *D*, densitometry analysis of three ligand blot experiments with α-Syn monomers (*C*) or multimers (*D*), respectively. A higher level of binding of WTS to cytoskeleton proteins as compared with different α-Syn variants was observed. Binding was stronger for α-Syn multimers than for monomers. *Bars*, mean intensity ± S.D. (*error bars*). *, $p < 0.05$.

the presence of WTS seeds (Fig. 3*D*). In line with this, the inhibitory effect of WTS seeds on Tau-promoted MT assembly was dose-dependent (Fig. 3, *H* and *I*). Tau-promoted MT assembly levels at 30 min in the presence of different amounts of WTS seeds normalized to control were found to decrease with increasing WTS concentrations (97.4% at 2.18 μM, 89.8% at 4.36 μM, 67.1% at 8.73 μM, and 36.7% at 17.45 μM; R^2 for a linear regression fit 0.9877, p value for regression 0.0006; Fig. 3*I*). At the same time, no dose dependence was observed for WTS monomers on Tau-promoted MT assembly (Fig. 3, *G* and *I*; R^2 for a linear regression fit 0.2416, p value for regression 0.4). These results indicate the potency of WTS seeds to interplay with Tau-controlled MT polymerization. α-Syn oligomeric and fibrillar forms did not influence this process.

α-Syn Oligomers but Not Fibrils Slow Down MT Gliding Velocity in Vitro—Because WTS, α-Syn variants, and different multimeric forms of α-Syn were able to bind to KIF5A as well as tubulin and MTs (Fig. 1), we aimed to investigate whether they are able to affect kinesin-MT interaction. To monitor the functionality of the kinesin-MT system, we took advantage of an *in vitro* gliding assay that mimics the anterograde axonal transport process (29). Monomers and multimers of WTS and α-Syn variants were added at a concentration of 10 μM (mimicking physiological conditions) (33, 34), and gliding of MTs across the KIF5A-coated surface was monitored by live imaging (Fig. 4*A*). Independently of the mutation, α-Syn monomers did not largely influence MT gliding (mean velocity ± S.D.: control, 0.85 ± 0.04 μm/s; WTS, 0.75 ± 0.07 μm/s; E57K, 0.77 ± 0.09 μm/s; A30P, 0.77 ± 0.09 μm/s; aSyn(30–110), 0.78 ± 0.07 μm/s; Fig. 4*D*). Intriguingly, among α-Syn multimers, only oligomers were able to influence the MT gliding character and velocity (Fig. 4, *B*, *C*, and *E*). The gliding MTs were straight in control and in the presence of WTS seeds, and α-Syn fibrils (control as representative for WTS seeds and α-Syn fibrils in Fig. 4, *B* and *C*; see supplemental Movie 1). In the presence of α-Syn oligomers, MTs were more likely bent (E57K in Fig. 4, *B* and *C*, and supplemental Movie 2) (data not shown). Moreover, α-Syn oligomers significantly decreased the gliding velocity of MTs (E57K (0.69 ± 0.08 μm/s) and A30P (0.64 ± 0.06 μm/s) *versus* control (0.85 ± 0.04 μm/s); $p < 0.05$; Fig. 4*E*). These data indicate impairment of kinesin-MT motility by α-Syn oligomers.

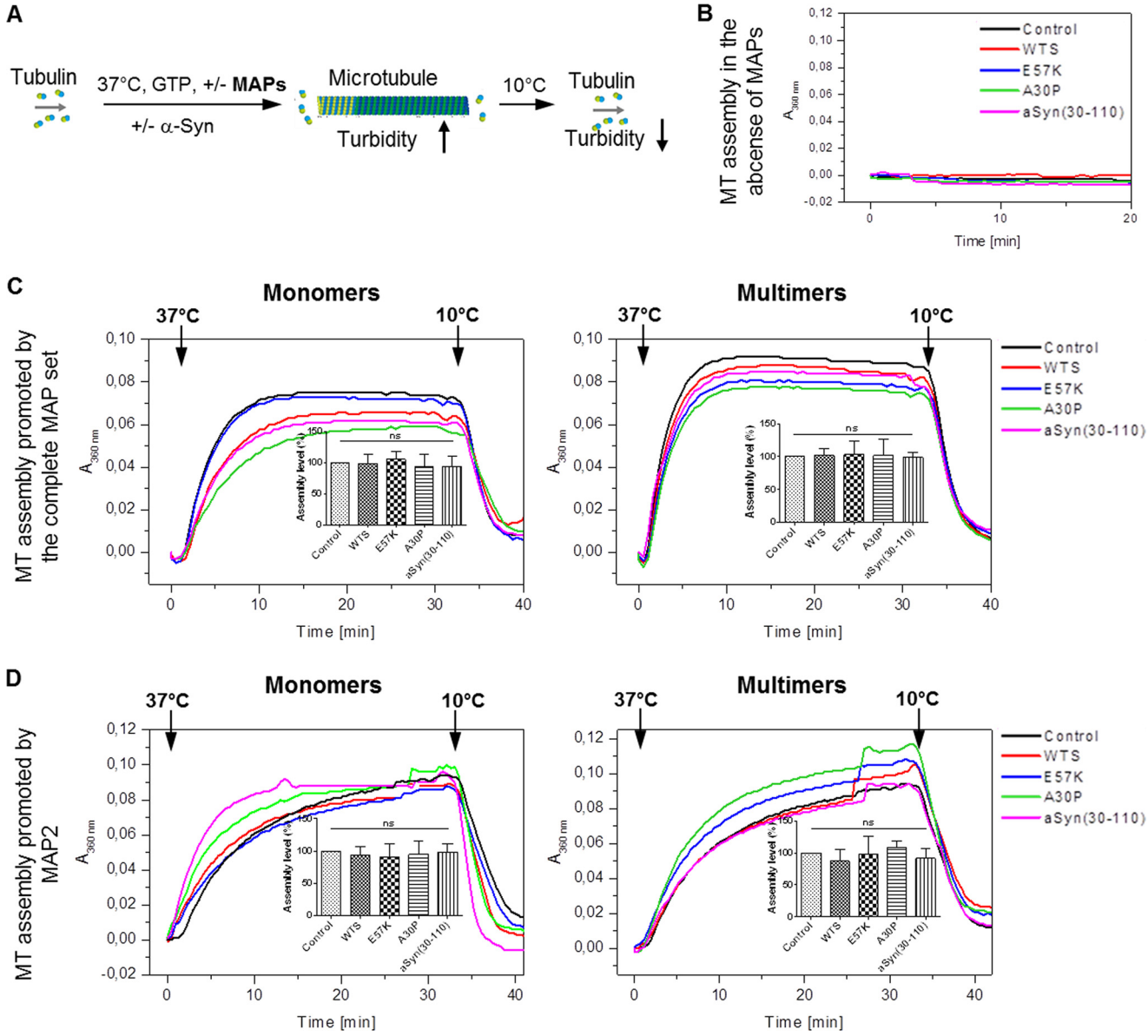

FIGURE 2. **α-Syns do not influence MT assembly in the presence of the complete MAP set and MAP2.** *A*, scheme of the *in vitro* MT assembly assay. MTs were formed from tubulin dimers in the presence of GTP and with or without MAPs at 37 °C accompanied by increasing turbidity of the solution. α-Syns were added to the MT assembly mixture to test for α-Syn-specific effect on MT formation. Cooling to 10 °C leads to disassembly of MT and to a turbidity decrease. *B*, negative controls of MT assembly. MTs were formed from tubulin dimers in the absence of MAPs. Monomers of α-Syn were added to test for their MAP-like activity. Purified tubulin was not able to assemble into MTs either in the absence of MAPs (*Control*) or with the addition of any of the α-Syn species. α-Syn does not have an intrinsic MAP-like activity. Representative measurements of three independent experiments are shown. *C*, MTs were formed from MTPs that consist of 80% tubulin and 20% set of MAP1, MAP2, and Tau in the presence of 4 μM WTS or α-Syn variants in either monomeric (*left*) or multimeric (*right*) form. Neither α-Syn monomers nor α-Syn multimers affected MT formation from MTP. *D*, MTs were assembled from tubulin in the presence of MAP2 and α-Syn monomers (*left*) or aSyn multimers (*right*) at a molecular ratio of α-Syn to MAP2 of 4. α-Syn proteins did not influence MAP2-promoted MT assembly. *C* and *D*, *insets* represent normalized MT assembly levels at the 30 min time point in the presence of monomers (*left* in *C* and *D*) or multimers (*right* in *C* and *D*) of α-Syn, respectively. Means of three independent measurements ± S.D. (*error bars*) are shown in the *insets*. In all cases, a control assay was performed in the absence of α-Syn. *ns*, not significant compared with control. Assembly reactions were cooled to 10 °C to induce destabilization of MT to test if α-Syn species can stabilize established MTs. α-Syn proteins did not have MT-stabilizing activity. Representative diagrams of three independent experiments are shown.

Overexpression of Oligomers of α-Syn Leads to Disrupted Neurite Morphology in a Dopaminergic Neuronal Cell Line—Our findings from the cell-free system show an inhibitory capacity of WTS seeds on Tau-promoted MT formation and α-Syn oligomer-mediated reduction of kinesin-MT gliding. The question arises of whether specific α-Syn species (seeds or oligomers) that critically affect MT-kinesin cytoskeleton *in vitro* would cause neurite pathology in neuronal cells. We therefore aimed to specifically investigate the influence of α-Syn seeds and oligomers on neurite morphology and the MT-kinesin system in a neuronal cell culture. Therefore, specifically WTS and E57K, as examples of seeds and oligomers, respectively, were chosen. They were overexpressed in LUHMES cells (a human dopaminergic neuronal cell line) using LV infection.

Different MOIs (2 and 4) were applied to achieve different levels of α-Syn overexpression. Confirming previous data, a high level of α-Syn overexpression (LV infection at MOI 4) resulted in increased cell death in E57K-infected neurons

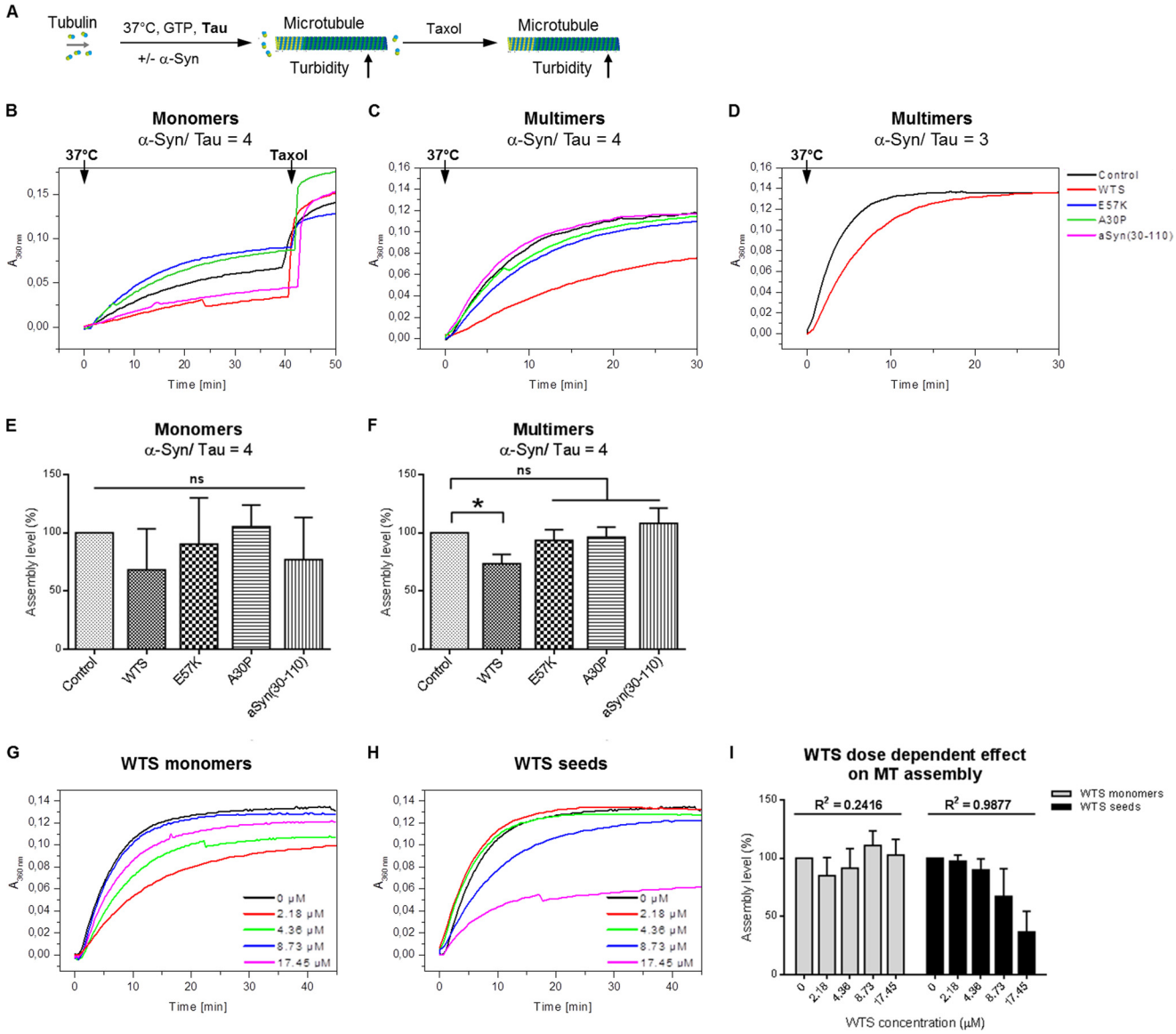

FIGURE 3. **WTS seeds significantly impair Tau-promoted MT assembly.** *A*, scheme of the *in vitro* MT assembly assay. MTs are formed from tubulin dimers in the presence of GTP and Tau at 37 °C accompanied by increasing turbidity of the solution. Turbidity assays were performed in the presence of α-Syn at α-Syn/Tau ratios of 4 or 3. In all cases, control was a turbidity assay performed in the absence of α-Syn. The MT assembly-promoting drug taxol was added to promote MT formation under inhibiting conditions. *B–D*, representative diagrams of three independent experiments with either α-Syn monomers (*B*) or α-Syn multimers (*C*) at an α-Syn/Tau ratio of 4 and with WTS seeds at an α-Syn/Tau ratio of 3 (*D*). WTS seeds, but not oligomers or fibrils and not WTS monomers, inhibited Tau-promoted MT assembly. Adding more Tau to the assay can rescue an inhibition of MT assembly caused by WTS seeds. Each *curve* represents one measurement. Taxol was added to each reaction with monomers to induce formation of MTs (40 min time point; *B*). Similarly, taxol increased turbidity when added to α-Syn multimeric assays (data not shown). *E* and *F*, normalized assembly levels calculated as turbidity values at the 30 min time point for WTS and each α-Syn variant in monomeric (*E*) or multimeric stage (*F*) at an α-Syn/Tau ratio of 4. The means of three independent measurements ± S.D. (*error bars*) are shown. Only WTS seeds significantly inhibited Tau-promoted MT formation. *, $p < 0.05$; *ns*, not significant. *G* and *H*, MTs were assembled from tubulin in the presence of Tau and different concentrations of WTS monomers (*G*) or WTS seeds (*H*). Each *curve* represents one measurement. Representative diagrams of three independent experiments are shown. *I*, WTS seeds but not monomers dose-dependently inhibited Tau-promoted formation of MTs. Normalized assembly levels calculated as turbidity values at the 30 min time point under different WTS concentrations as means of three independent measurements ± S.D. are shown. R^2, a linear regression coefficient.

(Fig. 5, *A* and *D*) (12, 13). Importantly, mild levels of α-Syn overexpression (WTS and E57K after LV infection at MOI 2) did not significantly increase neuronal cell toxicity (Fig. 5*B*). The following experiments were performed in LUHMES cells overexpressing mild levels of α-Syn (MOI 2).

First, LUHMES cells were analyzed for their neurite network morphology following LV infection. The overexpression of mild amounts of the oligomerizing α-Syn variant led to significant disruptions in the neurite network morphology compared with mock-infected cells (Fig. 5, *C* and *E*). Mild WTS overexpression also changed the neurite morphology, although this effect was not as pronounced as in E57K-overexpressing cells (Fig. 5, *C* and *E*). Potentiating a possible interplay of α-Syn seeds and oligomers with a neuritic MT-based system and in line with the *in vitro* MT assembly data, colocalization of α-Syn with β3-tubulin and Tau was present endogenously in mock-infected LUHMES cells and in LUHMES cells overexpressing WTS and E57K (Fig. 5, *F* and *G*).

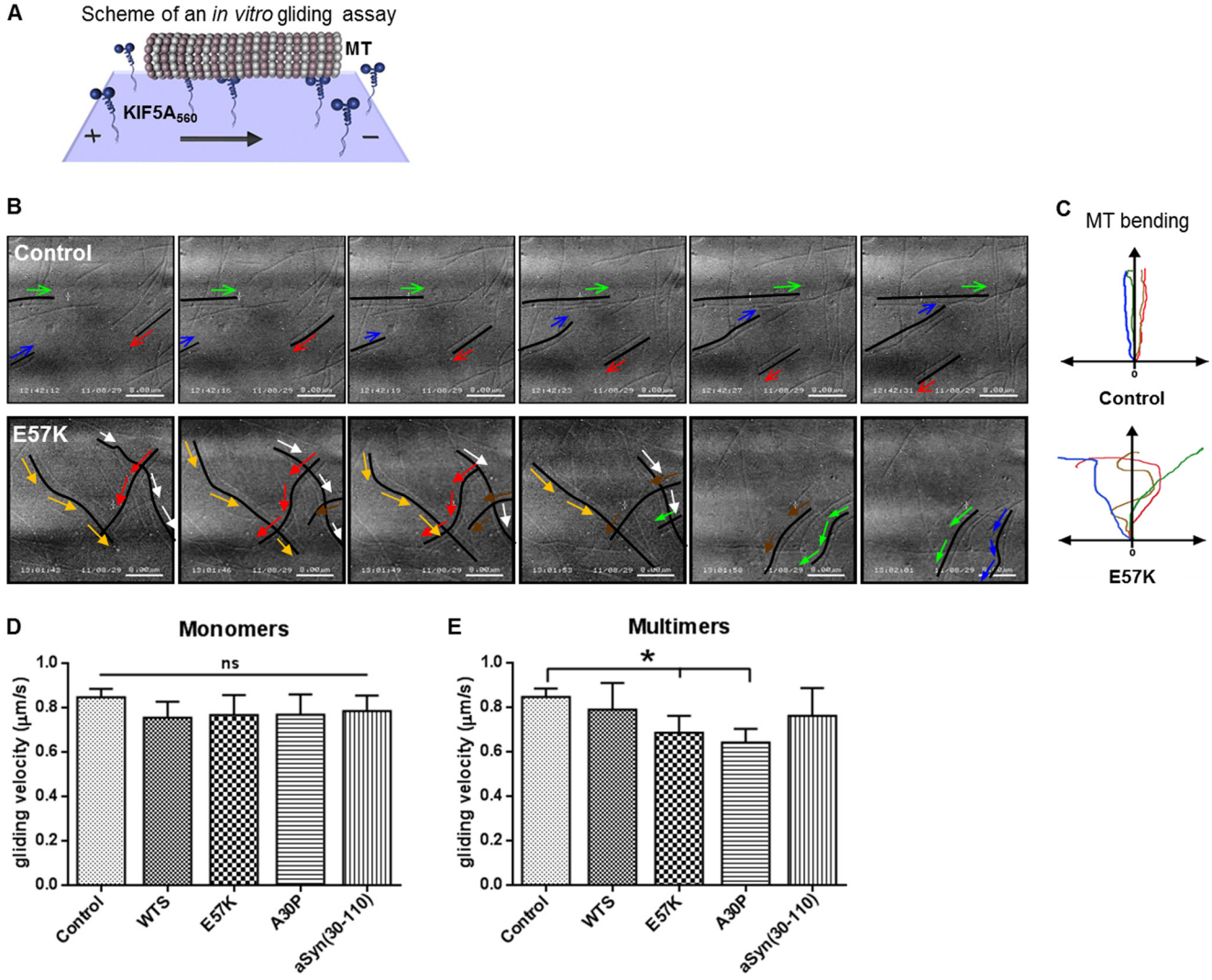

FIGURE 4. **MT gliding velocity *in vitro* is significantly impaired by α-Syn oligomers.** *A*, *in vitro* gliding assays were performed using $KIF5A_{560}$ and taxol-stabilized MTs in the presence of ATP. Monomeric or multimeric forms of WTS and α-Syn variants were added at a final concentration of 10 μM. The control gliding assay (*Control*) did not contain α-Syn. *B*, representative 3-s video sequences of a time lapse imaging of 19 s. *Color arrows* visualize movement directions of selected MTs that are visualized as *black lines* or *curves*. In a control condition, MTs were *directed lines* (*Control*; *top*), whereas MT movement was changing directions in the presence of oligomers (E57K; *bottom*). Respective representative videos are provided as supplemental material. *C*, a schematic summarizing MT gliding character in the absence (*Control*; *top*) and in the presence of α-Syn oligomers (*E57K*; *bottom*). The *y* axis shows a hypothetical MT movement direction, and *color lines* represent trajectories of individual MTs. *D* and *E*, mean gliding velocities ± S.D. (*error bars*) in the presence of WTS, α-Syn variants, and their multimers. Oligomers significantly reduced MT gliding velocity *in vitro* (E57K and A30P, respectively) (*E*). Three independent experiments were performed. Velocities of at least 10 MTs were measured in each experiment. *, $p < 0.05$; *ns*, not significant.

WTS and E57K α-Syn Reduce MT Stability and Alter KIF5-dependent Cargo Distribution in LUHMES Cells—To clarify whether the observed disruption of the neurite network morphology by α-Syn seeds and oligomers correlates with a dysfunction of the MT-based system, we investigated the stability of MTs and KIF5-dependent cargo distribution in neuronal cells mildly overexpressing WTS or E57K α-Syn. We therefore determined the amount of acetylated tubulin, as a measure of stabilized MTs. We found a significant reduction of acetylated tubulin in LUHMES cells overexpressing WTS and E57K compared with controls (Fig. 6, *A* and *D*, $p < 0.05$). Because the loss of tubulin acetylation was shown to decrease binding and motility of KIF5 (35), we next investigated KIF5 and KIF5-dependent cargo distribution within neurites. We detected decreased amounts of KIF5 within neurites of LUHMES cells overexpressing WTS and a further reduction in E57K-overexpressing cells compared with control LUHMES (Fig. 6, *B* and *E*), suggesting diminished KIF5/MT interaction in the presence of α-Syn seeds and oligomers in neurites. Moreover, we found significantly fewer mitochondria (a KIF5-dependent cargo) distributed within neurites of LUHMES cells overexpressing WTS and even fewer in E57K-overexpressing cells compared with control cells (Fig. 6, *C* and *F*). These data suggest that α-Syn seeds and, more significantly, oligomers impair MT stability and MT-kinesin functionality in neuronal cells, and this is associated with a disruption of the neurite network morphology.

DISCUSSION

The sequence of pathological events caused by α-Syn aggregation and the impact of different α-Syn species is still unknown. In the present study, the interplay between proteins involved in axonal transport and different species of α-Syn,

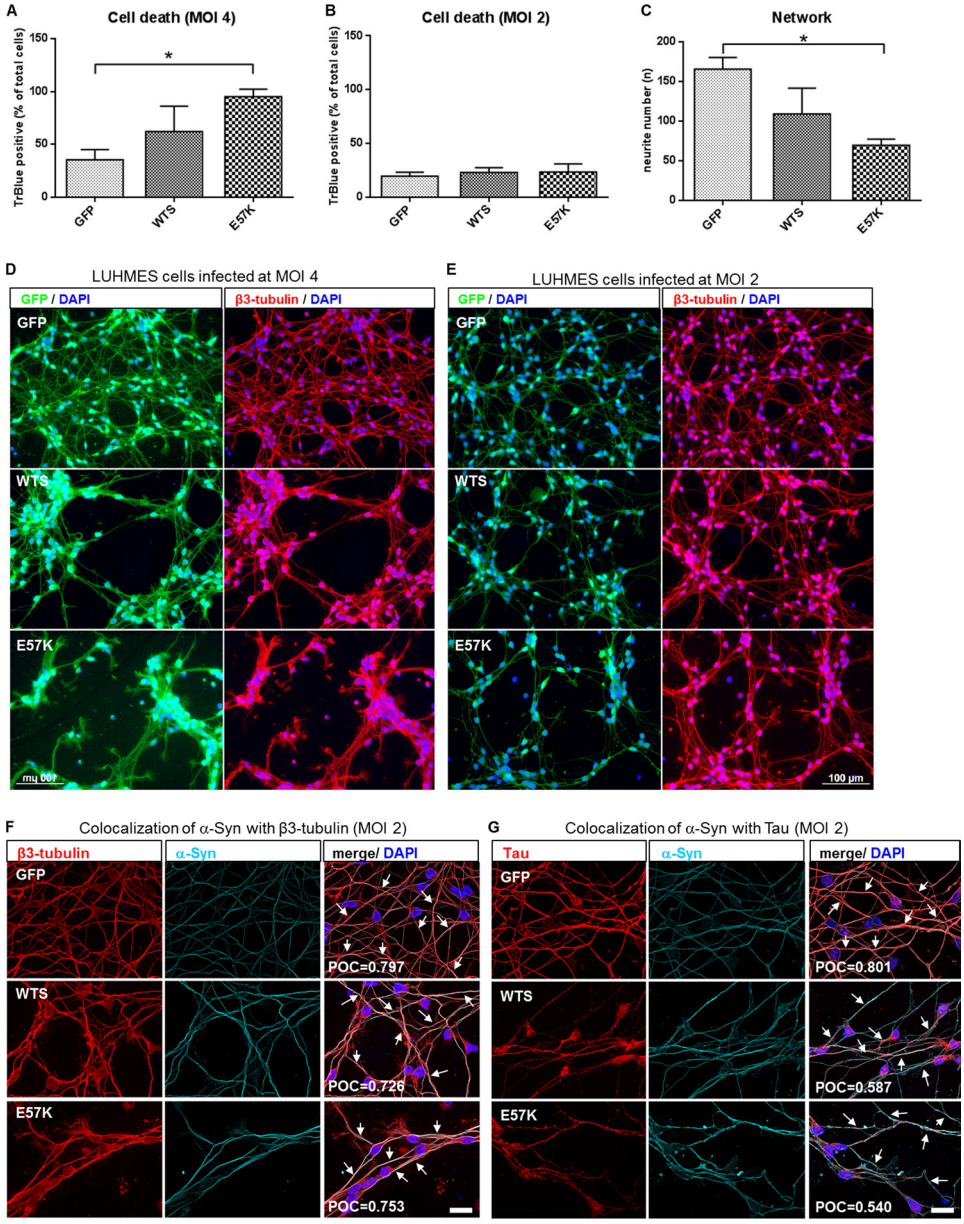

FIGURE 5. **Mild overexpression of E57K in a dopaminergic human neuronal cell line leads to impaired neurite morphology.** *A* and *B*, cell survival rates of LUHMES cells infected with lentiviruses expressing either GFP or α-Syn (WTS or E57K) at MOI 4 and MOI 2, respectively. High overexpression of WTS and E57K (MOI 4) (*A*) causes cell toxicity in neuronal cells. Mild levels of α-Syn overexpression (MOI 2) (*B*) do not significantly increase cell death. Cell death was determined at day 6 of differentiation as a percentage of trypan blue-positive cells within the total number of cells. Mean ± S.D. (*error bars*) of three independent experiments is shown. *, $p < 0.05$. *C*, quantification of the neurite network of LUHMES cells infected at MOI 2. E57K significantly disrupt neuronal network morphology. Neurite numbers were calculated as numbers of neurite crossing points with three parallel horizontal lines crossing images at given places. *, $p < 0.05$. *D* and *E*, fluorescence images of differentiating LUHMES cells (day 4) infected with lentiviruses expressing either GFP or α-Syn (WTS or E57K) at MOI 4 and MOI 2, respectively. GFP expression is shown in *green* (*left-hand panels* in *D* and *E*). Cells were stained with anti-β3-tubulin antibody (*red*), and nuclei were visualized using DAPI (*blue*; *right-hand panels* in *D* and *E*). At mild levels of α-Syn overexpression (MOI 2), the network morphology of LUHMES cells overexpressing E57K is markedly affected (*E*), whereas high levels of both WTS and E57K overexpression (MOI 4) cause strong neurite pathology (*D*). *Scale bars*, 100 μm. *F* and *G*, representative images of LUHMES cells infected with either GFP or α-Syn (WTS or E57K) LVs at MOI 2 and double-stained for β3-tubulin (*red*) and α-Syn (*cyan*) (*F*) or for Tau (*red*) and α-Syn (*cyan*) (*G*). Colocalization (*highlighted* with *arrows* on *merged images*) of α-Syn was detected with both β3-tubulin and Tau in all types of infected LUHMES cells, as determined by Pearson's overlap coefficient (*POC*). Pearson's overlap coefficient values shown represent a mean of three independent images. Nuclei were visualized using DAPI (*blue*). *Scale bars*, 20 μm.

such as oligomers (formed by A30P and E57K α-Syns), seeds (WTS), and fibrils (formed by aSyn(30–110)) was investigated. Our data show that WTS monomers and seeds bind to proteins required for MT-based anterograde axonal transport, such as KIF5A, tubulin, MTs, MAP2, and Tau. Interestingly, WTS seeds impaired MT polymerization *in vitro* promoted by axon-specific Tau protein in a dose-dependent manner. Moreover, in a model system of kinesin-driven transport, oligomers of α-Syn decreased kinesin-MT motility *in vitro*. In a human dopaminergic neuronal cell line, neurite network morphology was severely disrupted by mild overexpression of α-Syn oligomers. Neurite morphology disruption in these cells correlated with a significant reduction of MT stability and impaired amounts of KIF5 and KIF5-dependent cargo in neurites. Thus, our study

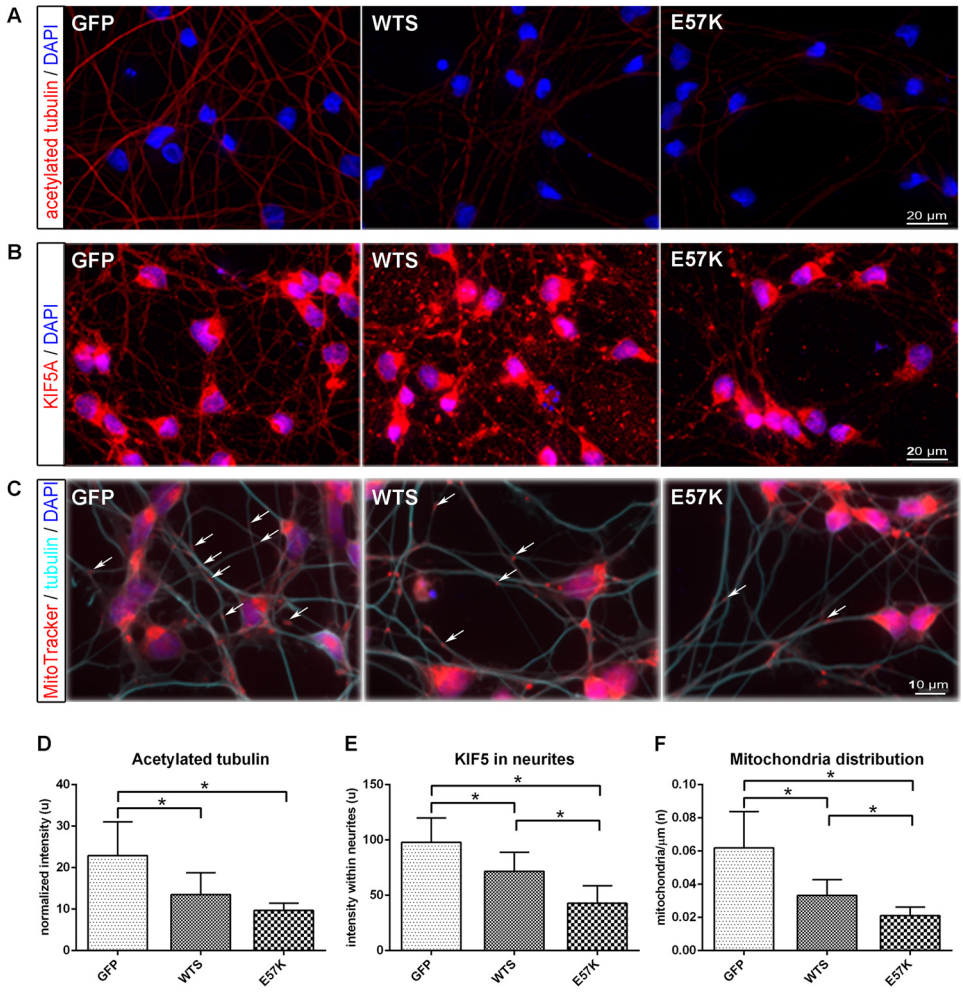

FIGURE 6. **Mild overexpression of WTS and E57K in dopaminergic human neuronal cells leads to impaired MT stability and KIF5-dependent cargo distribution.** *A–C*, fluorescence images of differentiating LUHMES cells (day 4) infected with lentiviruses expressing either GFP or α-Syn (WTS or E57K) at MOI 2, fixed with methanol, and stained for acetylated tubulin (*A*), KIF5 (*B*), and mitochondria and β3-tubulin (*C*). Note that the GFP signal is not detectable anymore after methanol fixation. *Scale bar*, 20 μm (*A* and *B*) and 10 μm (*C*). *D*, the level of acetylated tubulin, representing a portion of stabilized MTs, is significantly reduced in WTS- and E57K-overexpressing cells. Intensity values for acetylated tubulin were normalized to the numbers of DAPI-positive nuclei. *E*, KIF5 signal is impaired in neurites of WTS and even stronger in E57K neuronal cells. Signals are presented as mean intensity within single traced neurite ± S.D. (*error bars*) At least 100 neurites were analyzed for each cell type in three independent experiments. *F*, significantly fewer mitochondria are present within neurites of WTS-overexpressing and much fewer in E57K-overexpressing neuronal cells. Mitochondria are visualized using MitoTracker_RedCMXRos. The number of mitochondria was determined per 1 μm of neurite length. Some mitochondria are *highlighted* with *arrows*. *, $p < 0.05$.

describes complex interactions of α-Syn species with proteins involved in axonal transport and MT network, possibly underlying divergent toxic potentials of different α-Syn species.

The identification of proteins that interact with α-Syn may clarify the cellular processes accompanying α-Syn aggregation. Here, we observed a direct interaction of WTS with tubulin heterodimers, polymerized MTs, MAP2, Tau, and with the MT-based neuron-specific motor protein KIF5A, which confirms previous findings for tubulin (16, 22, 36–38) and expands data for Tau (39, 40), MAP2 (41), and KIF5A (42). In line with this, we observed a colocalization of α-Syn (WTS and E57K) with both Tau and tubulin in untreated and α-Syn-overexpressing LUHMES cells. The question raised is whether the binding capacity of α-Syn to cytoskeletal proteins is different between WTS and α-Syn variants. WTS and WTS seeds showed stronger binding to all tested cytoskeleton proteins compared with monomer and multimer fractions of the oligomer-promoting variants (E57K and A30P) and fibril-forming variant (aSyn(30–110)) of α-Syn. These results might suggest that alterations in axonal transport and/or MT networking could occur in the presence of α-Syn mutants. For example, familial PD mutants of α-Syn (A30P and A53T) were reported to favor formation of amorphous tubulin polymers lacking tubular structure in contrast to WTS *in vitro* (36).

Our study showed that WTS seeds, but not monomers or oligomers or fibrils of α-Syn, were able to reduce Tau-promoted MT polymerization. This is in line with a higher interacting capacity of WTS seeds compared with other forms of α-Syn proteins tested with tubulin, MTs, and Tau. Only Tau-promoted and not MAP2-promoted MT assembly was reduced by WTS seeds. The differences between MAP2- and Tau-directed effects of WTS seeds might highlight a preferential activity of α-Syn toward axon-specific proteins, such as Tau (40), compared with dendrite-specific proteins (MAP2). Because taxol was able to rescue MT polymerization to the control level, we hypothesized that WTS seeds did not cause irreversible

tubulin changes. Instead, this effect could be due to the interaction of WTS seeds and/or WTS-tubulin multimers with Tau molecules that might temporally and spatially separate Tau from MTs. This idea might be potentiated by the fact that adding more Tau to the assay could rescue an inhibitory effect of WTS seeds. Moreover, Tau and α-Syn can promote aggregation of each other (43, 44) and are colocalized in Lewy bodies in PD brains (45). Furthermore, α-Syn was reported to bind to the MT-binding domain of Tau and to promote Tau phosphorylation at Ser-262/356 and Ser-396/404 (40, 46), both of which would enhance the dissociation of Tau from MTs. Notably, a recent large scale replication study has confirmed a strong association of the Tau genetic locus (MAPT, rs2942168) with sporadic PD, further potentiating Tau involvement in the pathogenesis of PD (47).

Disruption of MT structures after overexpression of α-Syn was reported previously in different cellular systems (19, 22). Importantly, in our study, WTS overexpression in a neuronal cell line led to significant reduction of the acetylated tubulin level, indicating a loss of MT stability. Thus, our data provide evidence that α-Syn seeds might be the species that evoke MT dysfunction and destabilize MT networks under α-Syn-aggregating conditions. Interestingly, tubulin has been shown to promote α-Syn fibril formation, to form insoluble complexes with α-Syn in primary mouse neurons, and to colocalize with α-Syn in Lewy bodies (16, 20, 21). In turn, α-Syn seeds induce depolymerization of MTs and thereby increase the level of free tubulin. This might indicate that α-Syn aggregation-induced MT depolymerization and tubulin-induced/enhanced α-Syn seeding are interconnected.

MTs are important cytoskeletal filaments that control cellular processes in neurons, including neurite structure, intracellular transport of different cargoes, and neuronal cell maintenance (48). α-Syn aggregation has been shown to increase the amount of "vacant synapses" (49) and neuritic degeneration (19, 50) in α-Syn-overexpressing neurons. The reason for these events might be MT aberrations and/or MT-dependent transport disruption. Our study was designed to clarify whether and which α-Syn species could alter MT-based functionality. We show that, whereas α-Syn seeds led to critical disruption of MT assembly, α-Syn oligomers significantly slowed down MT gliding across the KIF5A-coated surface *in vitro*. Fibrils of α-Syn did not influence MT assembly and kinesin-dependant MT gliding. These data confirm previous findings of destructive effects of α-Syn oligomers and seeds on different cellular processes in contrast to "inert" fibrils (10, 11, 13, 51). In neurites of a neuronal cell line mildly overexpressing E57K, we found KIF5 significantly reduced. Previously, decreased KIF5A levels were reported at very early stages of PD (15) and in a rat PD model overexpressing A30P α-Syn mutant (52). In line with this, lower numbers of a KIF5-dependent cargo (mitochondria) in neurites of E57K-overexpressing cells might be a further indication for an α-Syn oligomer-induced transport disruption. An additional way of analyzing the effect of WTS and α-Syn variants on KIF5/MT interaction would be co-immunoprecipitation in neuronal cells. However, due to the ATP-dependant dynamic nature of the KIF5 interaction with MTs (35), we were not able to co-precipitate KIF5 with anti-tubulin antibody and *vice versa* (data not shown).

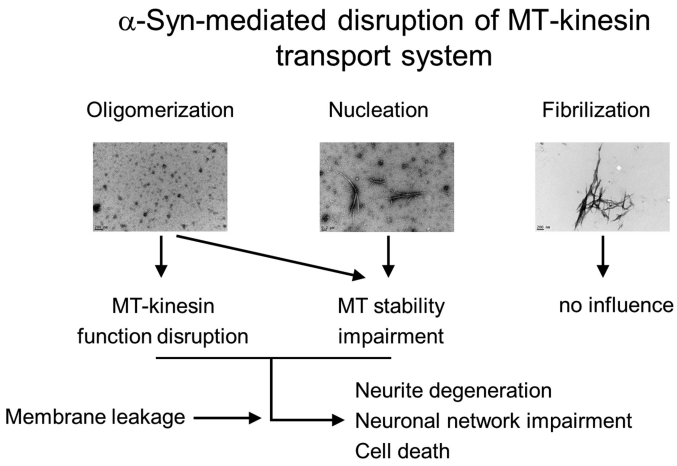

FIGURE 7. **Model of α-Syn aggregation-induced impairment of MT-based transport machinery.** As early pathological events in the course of α-Syn aggregation, α-Syn oligomers disrupt MT-kinesin function, and the presence of α-Syn seeds and oligomers critically influences MT network integrity. Together with other pathologic effects induced by α-Syn oligomers, such as membrane leakage, cytoskeleton changes might have a large spectrum of critical consequences that would together contribute to neurite degeneration, collapsed neuronal network, and finally to neuronal death. Fibrillar aggregates of α-Syn do not critically interfere with the axonal transport machinery and might represent "inert" α-Syn aggregate species.

Of interest, significantly reduced levels of acetylated tubulin were caused by mild overexpression of E57K in a neuronal cell line, showing disrupted MT stability. These data are in line with previous reports showing that α-Syn oligomers, when applied extracellularly, caused significant disruption of tubulin polymerization in a dopaminergic cell line (MES23.5), whereas no direct effect of α-Syn oligomers on MT assembly *in vitro* was seen in this study (23). Furthermore, overexpression of E57K led to more pronounced neurite degeneration and changes of neuronal network morphology than WTS. In both conditions, neurite degeneration occurred at lower expression levels than neuronal cell death. This might indicate a more direct critical influence of α-Syn oligomers on kinesin-MT interplay, whereas seeds of α-Syn would mostly act on MT network, destabilization of which would cause further alterations of MT-based transport.

In conclusion, we propose a sequence of pathologic events in neurites induced by α-Syn aggregation that involve impairment of MT-kinesin interaction and functionality due to α-Syn oligomers and MT network disruption by α-Syn oligomers and seeds. Oligomers and seeds then act together with other pathologic effects of α-Syn oligomers, such as membrane thinning and leakage (53) (Fig. 7), and together represent critical early mechanisms of synucleinopathies.

Acknowledgments—We thank Marina Wollmann, Theresa Halder, and Daniela Graef for excellent technical assistance and Marcel Leist for the LUHMES cells. We are grateful to Nada Ben Abdallah, Fred H. Gage, Roberto Japelli, Eliezer Masliah, Francesc Perez-Branguli, Michel Hadjihannas, and Jürgen Winkler for helpful discussions.

REFERENCES

1. Maroteaux, L., Campanelli, J. T., and Scheller, R. H. (1988) Synuclein. A neuron-specific protein localized to the nucleus and presynaptic nerve terminal. *J. Neurosci.* **8,** 2804–2815
2. Nemani, V. M., Lu, W., Berge, V., Nakamura, K., Onoa, B., Lee, M. K., Chaudhry, F. A., Nicoll, R. A., and Edwards, R. H. (2010) Increased expression of α-synuclein reduces neurotransmitter release by inhibiting synaptic vesicle reclustering after endocytosis. *Neuron* **65,** 66–79
3. Singleton, A. B., Farrer, M., Johnson, J., Singleton, A., Hague, S., Kachergus, J., Hulihan, M., Peuralinna, T., Dutra, A., Nussbaum, R., Lincoln, S., Crawley, A., Hanson, M., Maraganore, D., Adler, C., Cookson, M. R., Muenter, M., Baptista, M., Miller, D., Blancato, J., Hardy, J., and Gwinn-Hardy, K. (2003) α-Synuclein locus triplication causes Parkinson's disease. *Science* **302,** 841
4. Polymeropoulos, M. H., Lavedan, C., Leroy, E., Ide, S. E., Dehejia, A., Dutra, A., Pike, B., Root, H., Rubenstein, J., Boyer, R., Stenroos, E. S., Chandrasekharappa, S., Athanassiadou, A., Papapetropoulos, T., Johnson, W. G., Lazzarini, A. M., Duvoisin, R. C., Di Iorio, G., Golbe, L. I., and Nussbaum, R. L. (1997) Mutation in the α-synuclein gene identified in families with Parkinson's disease. *Science* **276,** 2045–2047
5. Krüger, R., Kuhn, W., Müller, T., Woitalla, D., Graeber, M., Kösel, S., Przuntek, H., Epplen, J. T., Schöls, L., and Riess, O. (1998) Ala30Pro mutation in the gene encoding α-synuclein in Parkinson's disease. *Nat. Genet.* **18,** 106–108
6. Zarranz, J. J., Alegre, J., Gómez-Esteban, J. C., Lezcano, E., Ros, R., Ampuero, I., Vidal, L., Hoenicka, J., Rodriguez, O., Atarés, B., Llorens, V., Gomez Tortosa, E., del Ser, T., Muñoz, D. G., and de Yebenes, J. G. (2004) The new mutation, E46K, of α-synuclein causes Parkinson and Lewy body dementia. *Ann. Neurol.* **55,** 164–173
7. Spillantini, M. G., Schmidt, M. L., Lee, V. M., Trojanowski, J. Q., Jakes, R., and Goedert, M. (1997) α-synuclein in Lewy bodies. *Nature* **388,** 839–840
8. Takeda, A., Mallory, M., Sundsmo, M., Honer, W., Hansen, L., and Masliah, E. (1998) Abnormal accumulation of NACP/α-synuclein in neurodegenerative disorders. *Am. J. Pathol.* **152,** 367–372
9. Haass, C., and Selkoe, D. J. (2007) Soluble protein oligomers in neurodegeneration. Lessons from the Alzheimer's amyloid β-peptide. *Nat. Rev. Mol. Cell Biol.* **8,** 101–112
10. Danzer, K. M., Haasen, D., Karow, A. R., Moussaud, S., Habeck, M., Giese, A., Kretzschmar, H., Hengerer, B., and Kostka, M. (2007) Different species of α-synuclein oligomers induce calcium influx and seeding. *J. Neurosci.* **27,** 9220–9232
11. Danzer, K. M., Ruf, W. P., Putcha, P., Joyner, D., Hashimoto, T., Glabe, C., Hyman, B. T., and McLean, P. J. (2011) Heat-shock protein 70 modulates toxic extracellular α-synuclein oligomers and rescues trans-synaptic toxicity. *FASEB J.* **25,** 326–336
12. Karpinar, D. P., Balija, M. B., Kügler, S., Opazo, F., Rezaei-Ghaleh, N., Wender, N., Kim, H. Y., Taschenberger, G., Falkenburger, B. H., Heise, H., Kumar, A., Riedel, D., Fichtner, L., Voigt, A., Braus, G. H., Giller, K., Becker, S., Herzig, A., Baldus, M., Jäckle, H., Eimer, S., Schulz, J. B., Griesinger, C., and Zweckstetter, M. (2009) Pre-fibrillar α-synuclein variants with impaired β-structure increase neurotoxicity in Parkinson's disease models. *EMBO J.* **28,** 3256–3268
13. Winner, B., Jappelli, R., Maji, S. K., Desplats, P. A., Boyer, L., Aigner, S., Hetzer, C., Loher, T., Vilar, M., Campioni, S., Tzitzilonis, C., Soragni, A., Jessberger, S., Mira, H., Consiglio, A., Pham, E., Masliah, E., Gage, F. H., and Riek, R. (2011) *In vivo* demonstration that α-synuclein oligomers are toxic. *Proc. Natl. Acad. Sci. U.S.A.* **108,** 4194–4199
14. Goldstein, A. Y., Wang, X., and Schwarz, T. L. (2008) Axonal transport and the delivery of pre-synaptic components. *Curr. Opin. Neurobiol.* **18,** 495–503
15. Chu, Y., Morfini, G. A., Langhamer, L. B., He, Y., Brady, S. T., and Kordower, J. H. (2012) Alterations in axonal transport motor proteins in sporadic and experimental Parkinson's disease. *Brain* **135,** 2058–2073
16. Alim, M. A., Hossain, M. S., Arima, K., Takeda, K., Izumiyama, Y., Nakamura, M., Kaji, H., Shinoda, T., Hisanaga, S., and Ueda, K. (2002) Tubulin seeds α-synuclein fibril formation. *J. Biol. Chem.* **277,** 2112–2117
17. Esteves, A. R., Arduíno, D. M., Swerdlow, R. H., Oliveira, C. R., and Cardoso, S. M. (2010) Microtubule depolymerization potentiates α-synuclein oligomerization. *Front. Aging Neurosci.* **1,** 5
18. Kim, M., Jung, W., Lee, I. H., Bhak, G., Paik, S. R., and Hahn, J. S. (2008) Impairment of microtubule system increases α-synuclein aggregation and toxicity. *Biochem. Biophys. Res. Commun.* **365,** 628–635
19. Lee, H. J., Khoshaghideh, F., Lee, S., and Lee, S. J. (2006) Impairment of microtubule-dependent trafficking by overexpression of α-synuclein. *Eur. J. Neurosci.* **24,** 3153–3162
20. Nakayama, K., Suzuki, Y., and Yazawa, I. (2009) Microtubule depolymerization suppresses α-synuclein accumulation in a mouse model of multiple system atrophy. *Am. J. Pathol.* **174,** 1471–1480
21. Nakayama, K., Suzuki, Y., and Yazawa, I. (2012) Binding of neuronal α-synuclein to β-III tubulin and accumulation in a model of multiple system atrophy. *Biochem. Biophys. Res. Commun.* **417,** 1170–1175
22. Zhou, R. M., Huang, Y. X., Li, X. L., Chen, C., Shi, Q., Wang, G. R., Tian, C., Wang, Z. Y., Jing, Y. Y., Gao, C., and Dong, X. P. (2010) Molecular interaction of α-synuclein with tubulin influences on the polymerization of microtubule *in vitro* and structure of microtubule in cells. *Mol. Biol. Rep.* **37,** 3183–3192
23. Chen, L., Jin, J., Davis, J., Zhou, Y., Wang, Y., Liu, J., Lockhart, P. J., and Zhang, J. (2007) Oligomeric α-synuclein inhibits tubulin polymerization. *Biochem. Biophys. Res. Commun.* **356,** 548–553
24. Volles, M. J., and Lansbury, P. T., Jr. (2007) Relationships between the sequence of α-synuclein and its membrane affinity, fibrillization propensity, and yeast toxicity. *J. Mol. Biol.* **366,** 1510–1522
25. Kalchishkova, N., and Böhm, K. J. (2008) The role of Kinesin neck linker and neck in velocity regulation. *J. Mol. Biol.* **382,** 127–135
26. Shelanski, M. L., Gaskin, F., and Cantor, C. R. (1973) Microtubule assembly in the absence of added nucleotides. *Proc. Natl. Acad. Sci. U.S.A.* **70,** 765–768
27. Weingarten, M. D., Lockwood, A. H., Hwo, S. Y., and Kirschner, M. W. (1975) A protein factor essential for microtubule assembly. *Proc. Natl. Acad. Sci. U.S.A.* **72,** 1858–1862
28. Herzog, W., and Weber, K. (1978) Fractionation of brain microtubule-associated proteins. Isolation of two different proteins which stimulate tubulin polymerization *in vitro*. *Eur. J. Biochem.* **92,** 1–8
29. Böhm, K. J., Steinmetzer, P., Daniel, A., Baum, M., Vater, W., and Unger, E. (1997) Kinesin-driven microtubule motility in the presence of alkaline-earth metal ions. Indication for a calcium ion-dependent motility. *Cell Motil. Cytoskeleton* **37,** 226–231
30. Scholz, D., Pöltl, D., Genewsky, A., Weng, M., Waldmann, T., Schildknecht, S., and Leist, M. (2011) Rapid, complete and large-scale generation of post-mitotic neurons from the human LUHMES cell line. *J. Neurochem.* **119,** 957–971
31. Sharon, R., Bar-Joseph, I., Frosch, M. P., Walsh, D. M., Hamilton, J. A., and Selkoe, D. J. (2003) The formation of highly soluble oligomers of α-synuclein is regulated by fatty acids and enhanced in Parkinson's disease. *Neuron* **37,** 583–595
32. Vilar, M., Chou, H. T., Lührs, T., Maji, S. K., Riek-Loher, D., Verel, R., Manning, G., Stahlberg, H., and Riek, R. (2008) The fold of α-synuclein fibrils. *Proc. Natl. Acad. Sci. U.S.A.* **105,** 8637–8642
33. Iwai, A., Masliah, E., Yoshimoto, M., Ge, N., Flanagan, L., de Silva, H. A., Kittel, A., and Saitoh, T. (1995) The precursor protein of non-Aβ component of Alzheimer's disease amyloid is a presynaptic protein of the central nervous system. *Neuron* **14,** 467–475
34. Seo, J. H., Rah, J. C., Choi, S. H., Shin, J. K., Min, K., Kim, H. S., Park, C. H., Kim, S., Kim, E. M., Lee, S. H., Lee, S., Suh, S. W., and Suh, Y. H. (2002) α-synuclein regulates neuronal survival via Bcl-2 family expression and PI3/Akt kinase pathway. *FASEB J.* **16,** 1826–1828
35. Reed, N. A., Cai, D., Blasius, T. L., Jih, G. T., Meyhofer, E., Gaertig, J., and Verhey, K. J. (2006) Microtubule acetylation promotes kinesin-1 binding and transport. *Curr. Biol.* **16,** 2166–2172
36. Alim, M. A., Ma, Q. L., Takeda, K., Aizawa, T., Matsubara, M., Nakamura, M., Asada, A., Saito, T., Kaji, H., Yoshii, M., Hisanaga, S., and Uéda, K. (2004) Demonstration of a role for α-synuclein as a functional microtubule-associated protein. *J. Alzheimer's Dis.* **6,** 435–442; discussion 443–439
37. Payton, J. E., Perrin, R. J., Clayton, D. F., and George, J. M. (2001) Protein-

protein interactions of α-synuclein in brain homogenates and transfected cells. *Brain Res. Mol. Brain Res.* **95,** 138–145
38. Wersinger, C., and Sidhu, A. (2005) Disruption of the interaction of α-synuclein with microtubules enhances cell surface recruitment of the dopamine transporter. *Biochemistry* **44,** 13612–13624
39. Esposito, A., Dohm, C. P., Kermer, P., Bähr, M., and Wouters, F. S. (2007) α-Synuclein and its disease-related mutants interact differentially with the microtubule protein Tau and associate with the actin cytoskeleton. *Neurobiol. Dis.* **26,** 521–531
40. Jensen, P. H., Hager, H., Nielsen, M. S., Hojrup, P., Gliemann, J., and Jakes, R. (1999) α-Synuclein binds to Tau and stimulates the protein kinase A-catalyzed Tau phosphorylation of serine residues 262 and 356. *J. Biol. Chem.* **274,** 25481–25489
41. D'Andrea, M. R., Ilyin, S., and Plata-Salaman, C. R. (2001) Abnormal patterns of microtubule-associated protein-2 (MAP-2) immunolabeling in neuronal nuclei and Lewy bodies in Parkinson's disease substantia nigra brain tissues. *Neurosci. Lett.* **306,** 137–140
42. Utton, M. A., Noble, W. J., Hill, J. E., Anderton, B. H., and Hanger, D. P. (2005) Molecular motors implicated in the axonal transport of Tau and α-synuclein. *J. Cell Sci.* **118,** 4645–4654
43. Geddes, J. W. (2005) α-Synuclein. A potent inducer of Tau pathology. *Exp. Neurol.* **192,** 244–250
44. Giasson, B. I., Forman, M. S., Higuchi, M., Golbe, L. I., Graves, C. L., Kotzbauer, P. T., Trojanowski, J. Q., and Lee, V. M. (2003) Initiation and synergistic fibrillization of Tau and α-synuclein. *Science* **300,** 636–640
45. Lee, V. M., Giasson, B. I., and Trojanowski, J. Q. (2004) More than just two peas in a pod. Common amyloidogenic properties of Tau and α-synuclein in neurodegenerative diseases. *Trends Neurosci.* **27,** 129–134
46. Duka, T., Duka, V., Joyce, J. N., and Sidhu, A. (2009) α-Synuclein contributes to GSK-3β-catalyzed Tau phosphorylation in Parkinson's disease models. *FASEB J.* **23,** 2820–2830
47. Sharma, M., Ioannidis, J. P., Aasly, J. O., Annesi, G., Brice, A., Van Broeckhoven, C., Bertram, L., Bozi, M., Crosiers, D., Clarke, C., Facheris, M., Farrer, M., Garraux, G., Gispert, S., Auburger, G., Vilariño-Güell, C., Hadjigeorgiou, G. M., Hicks, A. A., Hattori, N., Jeon, B., Lesage, S., Lill, C. M., Lin, J. J., Lynch, T., Lichtner, P., Lang, A. E., Mok, V., Jasinska-Myga, B., Mellick, G. D., Morrison, K. E., Opala, G., Pramstaller, P. P., Pichler, I., Park, S. S., Quattrone, A., Rogaeva, E., Ross, O. A., Stefanis, L., Stockton, J. D., Satake, W., Silburn, P. A., Theuns, J., Tan, E. K., Toda, T., Tomiyama, H., Uitti, R. J., Wirdefeldt, K., Wszolek, Z., Xiromerisiou, G., Yueh, K. C., Zhao, Y., Gasser, T., Maraganore, D., and Kruger, R. (2012) Large-scale replication and heterogeneity in Parkinson disease genetic loci. *Neurology* **79,** 659–667
48. De Vos, K. J., Grierson, A. J., Ackerley, S., and Miller, C. C. (2008) Role of axonal transport in neurodegenerative diseases. *Annu. Rev. Neurosci.* **31,** 151–173
49. Scott, D. A., Tabarean, I., Tang, Y., Cartier, A., Masliah, E., and Roy, S. (2010) A pathologic cascade leading to synaptic dysfunction in α-synuclein-induced neurodegeneration. *J. Neurosci.* **30,** 8083–8095
50. Winner, B., Regensburger, M., Schreglmann, S., Boyer, L., Prots, I., Rockenstein, E., Mante, M., Zhao, C., Winkler, J., Masliah, E., and Gage, F. H. (2012) Role of α-synuclein in adult neurogenesis and neuronal maturation in the dentate gyrus. *J. Neurosci.* **32,** 16906–16916
51. Luk, K. C., Song, C., O'Brien, P., Stieber, A., Branch, J. R., Brunden, K. R., Trojanowski, J. Q., and Lee, V. M. (2009) Exogenous α-synuclein fibrils seed the formation of Lewy body-like intracellular inclusions in cultured cells. *Proc. Natl. Acad. Sci. U.S.A.* **106,** 20051–20056
52. Chung, C. Y., Koprich, J. B., Siddiqi, H., and Isacson, O. (2009) Dynamic changes in presynaptic and axonal transport proteins combined with striatal neuroinflammation precede dopaminergic neuronal loss in a rat model of AAV α-synucleinopathy. *J. Neurosci.* **29,** 3365–3373
53. Reynolds, N. P., Soragni, A., Rabe, M., Verdes, D., Liverani, E., Handschin, S., Riek, R., and Seeger, S. (2011) Mechanism of membrane interaction and disruption by α-synuclein. *J. Am. Chem. Soc.* **133,** 19366–19375